

B-site disordering in $\text{Pb}(\text{Sc}_{1/2}\text{Ta}_{1/2})\text{O}_3$ by mechanical activation

X. S. Gao, J. M. Xue, and J. Wang^{a)}

Department of Materials Science, National University of Singapore, Singapore 117543

T. Yu and Z. X. Shen

Department of Physics, National University of Singapore, Singapore 119260

(Received 2 January 2003; accepted 17 April 2003)

B-site disorder in $\text{Pb}(\text{Sc}_{1/2}\text{Ta}_{1/2})\text{O}_3$ (PST) is traditionally tailored by thermal annealing after sintering at elevated temperatures. In this letter, we report B-site disordering in PST triggered by mechanical activation (MA), and the resulting ferroelectric behaviors thus derived. MA induces B-site order–disorder transformation in PST, and more interestingly, the structural disorder can well be retained in sintered PST, leading to a change in ferroelectric transition behavior (e.g., from a normal ferroelectric to relaxor) and a shift in Curie temperature. A designed degree of disorder in PST can therefore be obtained by the effective combination of presinter MA and subsequent sintering, giving rise to the specific ferroelectric properties that are required for certain applications.

© 2003 American Institute of Physics. [DOI: 10.1063/1.1581384]

In complex $\text{A}(\text{B}'\text{B}'')\text{O}_3$ perovskite structures, B-site cation order–disorder transformation can occur, leading to a dramatic change in the ferroelectric behaviors of relaxor ferroelectrics.¹ By controlling the degree of B-site disorder, ferroelectric properties of $\text{Pb}(\text{Sc}_{1/2}\text{Ta}_{1/2})\text{O}_3$ (PST) can be tailored to meet specifically designed applications.² Investigations into the order–disorder transformation in relaxors have led to understanding on the physical origins responsible for the observed ferroelectric behaviors.^{2–8} To realize a designed degree of structural disorder in relaxors, previous studies have been focused on partial substitutions for either B-site or A-site cations by certain dopants.^{9,10} Alternatively, it was achieved by an appropriate postsinter thermal annealing.¹¹ In several previous studies, $\text{Pb}(\text{Sc}_{1/2}\text{Ta}_{1/2})\text{O}_3$ was selected for studying B-site disorder and electric properties that were brought about by thermal annealing of quenched ceramic bodies from high sintering temperatures.^{5–7,11–13} However, thermal annealing at elevated temperatures can lead to formation of other structural defects, such as Pb vacancies as a result of loss of PbO .^{5–7,13} In a completely different approach, we report in this letter the order–disorder transformation in $\text{Pb}(\text{Sc}_{1/2}\text{Ta}_{1/2})\text{O}_3$ triggered by mechanical activation, where the structural disorders can be retained in sintered PST.

PST of ordered perovskite structure was synthesized via the Wolframite route,¹⁴ using PbO (>99%, J.T. Baker Inc.), Sc_2O_3 (99.6%, J.T. Baker Inc) and Ta_2O_5 (>99%, Aldrich) as the starting materials. They were then subjected to mechanical activation (MA) for various time periods in high-energy shake mill (SPEX 8000), which were designed to generate varying degrees of B-site disorder. Upon completion of MA, each PST composition was pressed into pellets and then sintered at 1200 °C for 4 h in an enclosed crucible with powder bedding to minimize the PbO loss. Structural evolution and variation in the degree of B-site order were monitored by x-ray diffraction (XRD) ($\text{Cu K}\alpha$, X'pertTM

Diffraction, Phillips) and Raman spectroscopic studies (SpexTM T64000, Jobin-Yvon).¹² Dielectric properties were characterized using a precision LCR meter (HP 4284A).

Figure 1(a) shows the XRD traces of PST derived via the Wolframite route and then subjected to various hours of MA. The cubic structure of PST is clearly indicated by the diffraction peak at 2θ of 21.7° of the (002) plane, while the peak at 2θ of 18.8° of (111) superlattice indicates the degree of B-site order. With increasing MA time, the superlattice peak became weakened and had almost completely disappeared upon MA for 6 h. At the same time, there was an apparent

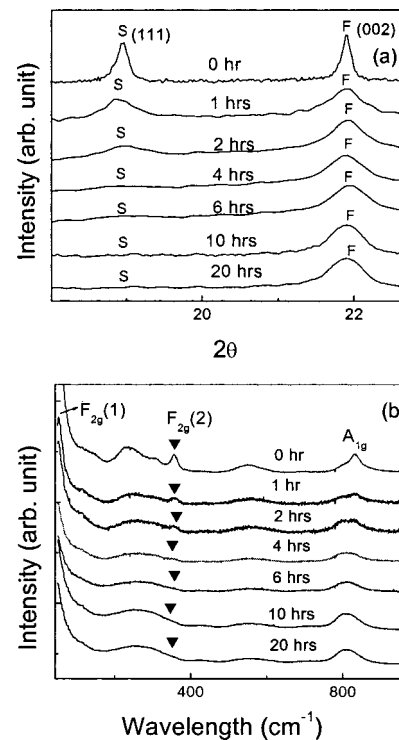


FIG. 1. (a) XRD traces and (b) Raman spectra for PST subjected to various hours MA. S: (111) superlattice diffraction originated from B-site cation order, and F: the fundamental diffraction of perovskite structure. ▼: Raman $F_{2g}(2)$ band indicating B-site cation order.

^{a)} Author to whom correspondence should be addressed; electronic mail: maswangj@nus.edu.sg

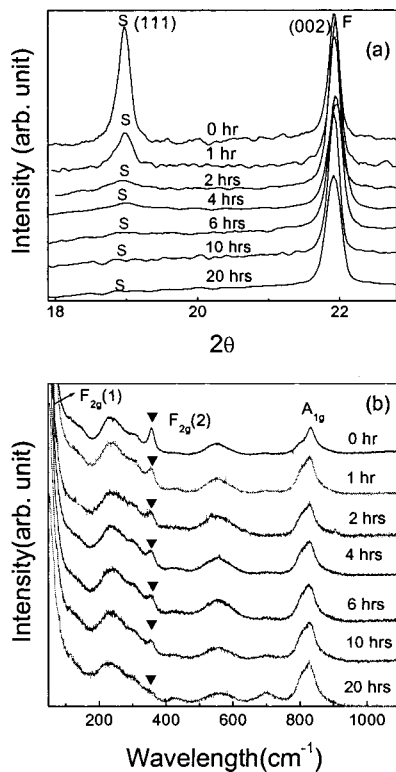


FIG. 2. (a) XRD traces and (b) Raman spectra for PST subjected to various hours of MA and subsequently sintered at 1200 °C for 4 h. S:(111) superlattice diffraction patterns, and F: the fundamental diffraction peak. ▼: Raman $F_{2g}(2)$ band indicating the B-site cation order.

broadening of the cubic (002) and (111) peaks, implying a refinement in both crystalline and ordering domain sizes. The order–disorder transformation triggered by MA was also clearly reflected in Raman spectra as shown in Fig. 1(b). The bands at around 60, 358, and 832 cm^{-1} , which are assigned to $F_{2g}(1)$, $F_{2g}(2)$, and A_{1g} , respectively, are related to the $Fm3m$ space group in PST.^{15–17} In particular, $F_{2g}(2)$ peak is originated from the B-site order and can be used to represent the degree of B-site order. As illustrated in Fig. 1(b), $F_{2g}(2)$ diminishes quickly in band intensity with increasing MA time and has almost completely disappeared upon 10 h of MA, consistent with the XRD results.

More interestingly, as shown in Fig. 2(a), the B-site disorder generated by presinter MA in the fine PST particles cannot be eliminated by sintering at 1200 °C, which is a typical sintering schedule for PST, although there is a notable buildup in the structure order, as indicated by (111) superlattice peak. The B-site disorder retained in sintered PST was also confirmed by Raman spectroscopic studies as shown in Fig. 2(b), where the relative intensity of $F_{2g}(2)$ of PST sintered at 1200 °C for 4 h decreases with increasing presinter MA duration.

The phenomena observed in PST are very much different from the order–disorder transformation in $\text{Pb}(\text{Mg}_{1/3}\text{Nb}_{2/3})\text{O}_3$ – $\text{Pb}(\text{Mg}_{1/2}\text{W}_{1/2})\text{O}_3$ triggered by MA,¹⁷ where the structural order can easily be recovered by annealing at 900 °C. In PST sintered at 1200 °C, the degree of B-site order is strongly affected by the number of MA hours prior to sintering. Such unexpected retention of B-site disorder in sintered ceramic body creates an excellent opportunity for synthesizing PST with a designed degree of B-site disorder.

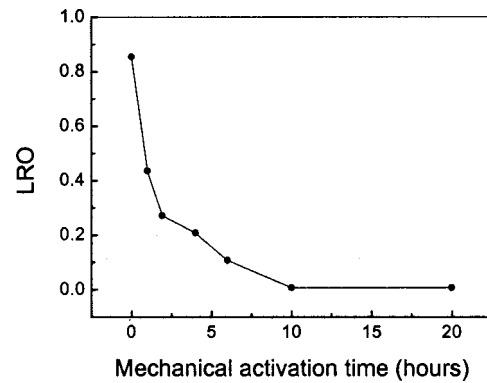


FIG. 3. LRO in sintered PST as a function of MA time prior to the high-temperature sintering at 1200 °C.

der, by an appropriate combination of MA and subsequent sintering at a normal sintering temperature. Figure 3 plots the degree of long-range order (LRO) in sintered PST, as calculated on the basis of peak intensity ratio of (200) plane to that of superlattice (111).¹² The B-site order disappears quickly at the initial few hours of MA, and a more-or-less completely disordered structure is generated after MA for 6 h.

B-site disorder in sintered PST has a dramatic effect on its dielectric properties. Figure 4 plots the dielectric constant as a function of temperature for PSTs subjected to various hours of MA prior to sintering at 1200 °C. As expected, PST without any presinter MA exhibits a dielectric peak at 20.3 °C with little frequency dispersion. This is apparently due to its ordered structure, as confirmed by both XRD and Raman studies. One hour of MA prior to sintering led to a shift in the dielectric peak towards lower temperature, together with a notable frequency dispersion. With increasing MA time, an apparent frequency dispersion is observed, and at the same time there is a sharp rise in the peak dielectric constant. The enhanced frequency dispersion and widened dielectric peak brought about by presinter MA demonstrate the relaxor behavior in association with the structural disorder in PST. Relaxor to normal ferroelectric (R–nFE) phase transition is indeed observed in PST derived from the intermediate hours of MA.

To further explore the variation in phase transition behavior brought about by MA in sintered PST, the reversal of

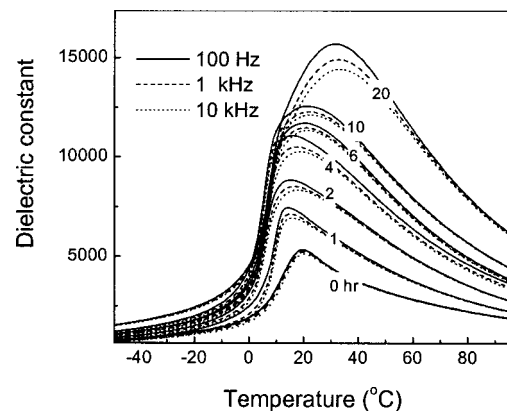


FIG. 4. Dielectric constants as a function of temperature for PST derived from various hours of MA and subsequently sintered at 1200 °C for 4 h, at three different frequencies.

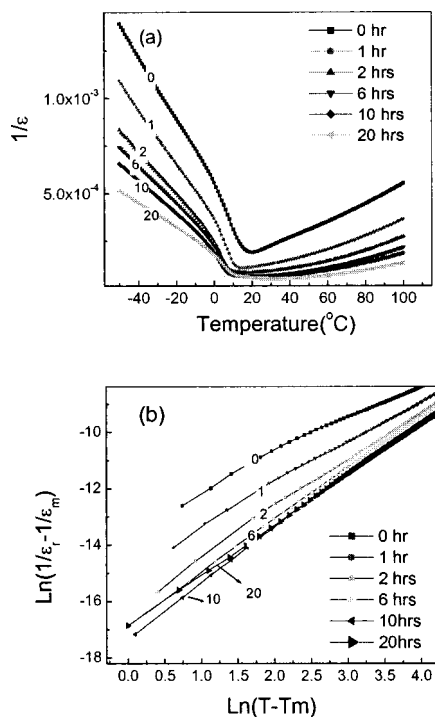


FIG. 5. (a) Reversal of dielectric constant as a function of temperature and (b) $\ln(1/\epsilon - 1/\epsilon_m)$ vs $\ln(T - T_m)$ plot for PSTs derived from various hours of MA and then sintered at 1200 $^{\circ}\text{C}$.

dielectric constant is plotted in Fig. 5(a) as a function of temperature. The more-or-less linear relationship at above Curie temperature for PST without any presinter MA suggests that it is a normal ferroelectric material. An apparent deviation from linear relationship is observed in PST subjected to presinter MA. Furthermore, the degree of deviation increases with increasing MA time, due to the buildup of B-site disorder. The B-site disorder in sintered PST is also illustrated by the plot of $\ln(1/\epsilon - 1/\epsilon_m)$ versus $\ln(T - T_m)$, as shown in Fig. 5(b), where ϵ , ϵ_m and T_m denote the dielectric constant, peak dielectric constant, and peak dielectric temperature, respectively. As expected, PST without any presinter MA and those subjected to a limited period of presinter MA do not exhibit a linear relationship in the plots. With increasing MA time (i.e., at >6 h), it approaches that of a typical relaxor ferroelectric above dielectric maximum temperature, which fits into $\ln(1/\epsilon - 1/\epsilon_m) = 1/(T - T_m)^{\delta}$ (δ is the relaxor factor).

When the particle size is refined into nanometer scale, it can strongly affect the phase transition and ferroelectric properties of PST.¹⁸ Although MA led to a dramatic fall in the average particle size of the PST powder, the grain size of

sintered PST is much beyond the nanometer scales. For example, an average particle size of 1.3, 1.7, 3.0, and 3.5 μm was measured for the PST sintered at 1200 $^{\circ}\text{C}$ that was mechanically activated for 2, 6, 10, and 20 h, respectively. Therefore, on the one hand, the disordering and dielectric behaviors in association with presinter MA in sintered PST are not due to particle size effect. On the other hand, MA of the PST powder significantly enhances its sintering behavior. For example, a sintered density of 93.1% theoretical at 1200 $^{\circ}\text{C}$ for 4 h for the PST subjected to 20 h of MA is compared favorably with 83.5% theoretical for the PST without any presinter mechanical activation.

In summary, mechanical activation triggers B-site order-disorder transformation in PST of perovskite structure, where the B-site disorder created by MA cannot be eliminated by normal sintering at high temperatures, and it is thus retained in sintered ceramics. The degree of disorder in sintered PST can therefore be tailored by a combination of presinter mechanical activation and subsequent sintering. By controlling the presinter MA duration, transition from a normal ferroelectric to a typical relaxor ferroelectric in PST is demonstrated in this letter. Accordingly, varying dielectric behavior and phase transition are realized in PST via a completely different approach from the traditional quenching and then postsinter annealing.

This paper is based upon work supported by the Science and Engineering Research Council, Singapore, under Grant No. 012 101 0130. The authors also acknowledge the support of the National University of Singapore.

- ¹C. A. Randall and A. S. Bhalla, *Jpn. J. Appl. Phys.* **29**, 327 (1990).
- ²L. E. Cross, *Ferroelectrics* **76**, 241 (1987).
- ³P. K. Davies and M. A. Akbas, *J. Phys. Chem. Solids* **61**, 159 (2000).
- ⁴Z. G. Ye, *Ferroelectrics* **184**, 193 (1996).
- ⁵F. Chu and N. Setter, *J. Appl. Phys.* **74**, 5129 (1993).
- ⁶F. Chu, I. M. Reany, and N. Setter, *J. Appl. Phys.* **77**, 1671 (1995).
- ⁷D. Viehland and J. F. Li, *J. Appl. Phys.* **75**, 1705 (1994).
- ⁸A. A. Bokov and Z.-G. Ye, *Phys. Rev. B* **66**, 1031 (2002).
- ⁹M. P. Harmer, J. Chen, P. Peng, H. M. Chan, and D. M. Smyth, *Ferroelectrics* **97**, 263 (1989).
- ¹⁰N. de Mathan, E. Husson, P. Gaucher, and A. Morell, *Mater. Res. Bull.* **25**, 427 (1990).
- ¹¹C. G. F. Stenger and A. J. Burggraaf, *Phys. Status Solidi A* **61**, 275 (1980).
- ¹²N. Setter and L. E. Cross, *J. Appl. Phys.* **51**, 4356 (1980).
- ¹³C. C. F. Stenger, F. L. Scholten, and A. J. Burggraaf, *Solid State Commun.* **32**, 989 (1979).
- ¹⁴S. L. Swartz and T. R. Shrout, *Mater. Res. Bull.* **17**, 1245 (1982).
- ¹⁵N. Setter and I. Laulicht, *Appl. Spectrosc.* **41**, 526 (1987).
- ¹⁶I. G. Siny, R. S. Katiyar, and A. S. Bhalla, *J. Raman Spectrosc.* **29**, 385 (1998).
- ¹⁷X. S. Gao, J. M. Xue, T. Yu, Z. X. Shen, and J. Wang, *J. Am. Ceram. Soc.* **85**, 833 (2002).
- ¹⁸Y. Park and K. M. Knowles, and K. Cho, *J. Appl. Phys.* **83**, 5702 (1999).